Spectrochimica Acta Part A: Molecular and Biomolecular Spectroscopy 104 (2013) 468–476

Contents lists available at SciVerse ScienceDirect

Spectrochimica Acta Part A: Molecular and Biomolecular Spectroscopy

journal homepage: www.elsevier.com/locate/saa

# Design, spectral characterization and biological studies of transition metal(II) complexes with triazole Schiff bases

Muhammad Hanif, Zahid H. Chohan *

*Department of Chemistry, Bahauddin Zakariya University, Multan 60800, Pakistan*

## HIGHLIGHTS

- Novel series of triazole derived Schiff bases and their transition metal complexes are studied.
- Characterization is made on the basis of their physical, spectral and analytical data.
- Antibacterial and antifungal correlation with the metal ions is established.
- *In vitro* antibacterial and antifungal activity is enhanced upon coordination.

## GRAPHICAL ABSTRACT

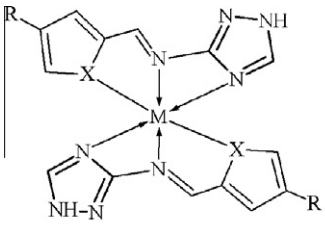


X = N R= H , X= S R= Br

M= Co(II), Ni(II), Cu(II) and Zn(II)

## ARTICLE INFO

*Article history:*
Received 20 September 2012
Received in revised form 8 November 2012
Accepted 23 November 2012
Available online 4 December 2012

*Keywords:*
Triazole Schiff bases
Metal(II) complexes
Antibacterial
Antifungal activities

## ABSTRACT

A new series of three biologically active triazole derived Schiff base ligands $\mathbf{L^1}$–$\mathbf{L^3}$ have been synthesized in equimolar reaction of 3-amino-1*H*-1,2,4-triazole with pyrrol-2-carboxaldehyde, 4-bromo-thiophene-2-carboxaldehyde, and 5-iodo-2-hydroxy benzaldehyde. The prepared Schiff bases were used for further complex formation reaction with different metal elements like Co(II), Ni(II), Cu(II) and Zn(II) as chlorides by using a molar ratio of ligand:metal as 2:1. The structure and bonding nature of all the compounds were identified by their physical, spectral and analytical data. All the metal(II) complexes possessed an octahedral geometry except the Cu(II) complexes which showed a distorted octahedral geometry. All the synthesized compounds, were studied for their *in vitro* antibacterial, and antifungal activities, against four Gram-negative (*Escherichia coli*, *Shigella sonnei*, *Pseudomonas aeruginosa* and *Salmonella typhi*) and two Gram-positive (*Bacillus subtilis* and *Staphylococcus aureus*) bacterial strains and against six fungal strains (*Trichophyton longifusus*, *Candida albicans*, *Aspergillus flavus*, *Microsporum canis*, *Fusarium solani* and *Candida glabrata)* by using agar-well diffusion method. It has been shown that all the synthesized compounds showed moderate to significant antibacterial activity against one or more bacterial strains. *In vitro* Brine Shrimp bioassay was also carried out to investigate the cytotoxic properties of these compounds. The data also revealed that the metal complexes showed better activity than the ligands due to chelation/coordination.



## Introduction

Triazoles and their derivatives occupy a central position in modern heterocyclic chemistry due to their biologically active nature. These compounds constitute heterocyclic groups that are commonly incorporated into compounds of pharmaceutical interest [1]. Triazole compounds such as fluconazole is a broad spectrum antifungal [2], trazodone is used as an antidepressant [3] vorozole, anastrozole and letrozole are potentially used to inhibit breast cancer [4]. It is evident that the azomethine linkage (C=N) is an essential structural requirement for biological activity [5]. Several azomethine group containing compounds have been reported to possess remarkable antibacterial [6], antifungal [7] and

* Corresponding author. Tel.: +92 3006802791.
*E-mail address:* dr.zahidchohan@gmail.com (Z.H. Chohan).

1386-1425/$ - see front matter © 2012 Elsevier B.V. All rights reserved.
http://dx.doi.org/10.1016/j.saa.2012.11.077

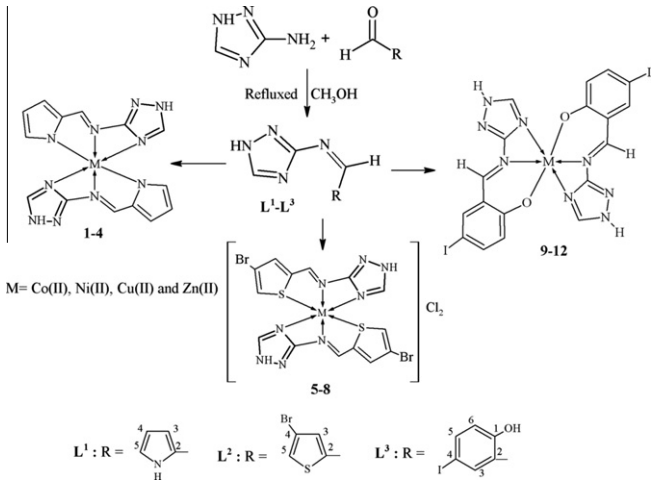


**Scheme 1.** Preparation of the ligands $\mathbf{L^1}$–$\mathbf{L^3}$ and their metal complexes **1**–**12.**

anticancer activities [8]. In view of above mention, biological behavior of triazole and azomethine linkage (C═N) many triazole based Schiff bases have also been reported to possess antibacterial [9], antifungal [10], antitumor [11], plant growth regulating [12] and cytotoxic [13] activities. It is also known that N and S atoms play a key role in the coordination of metals at the active sites of numerous biomolecules. Metallo-organic chemistry is becoming an emerging area of research due to the demand for new metal-based antibacterial and antifungal compounds [13–15]. Various investigations have proved that binding of a drug to a metalloelement enhances its activity and in some cases, the complex possesses even more healing properties than the parent drug [16]. In the present studies metalloelement such as copper, cobalt, nickel and zinc have been focused due to their smaller size and comparatively higher nuclear charge and thus have a great affinity to form coordination compounds. A bulk of literature [17–20] reveals that upon coordination with these metalloelements biologically inactive compounds become active and less biologically active compounds become more active.

In view of the significant structural and biological applications of triazole compounds, we wish to report the synthesis of a new class of triazole Schiff base derivatives $\mathbf{L^1}$–$\mathbf{L^3}$, from the condensation reaction of 3-amino-1,2,4-triazole with 1*H*-pyrrole-2-carboxaldehyde, 4-bromo-thiophene-2-carboxaldehyde and 5-iodo-2-hydroxybenzaldehydes respectively, and their cobalt(II), nickel(II), copper(II) and zinc(II) metal complexes **1**–**12** (Scheme 1). These compounds have been investigated for *in vitro* antibacterial activity against four Gram-negative (*Escherichia coli*, *Shigella sonnei*, *Pseudomonas aeruginosa*, *Salmonella typhi*) and two Gram-positive (*Staphylococcus aureus*, *Bacillus subtilis*) bacterial strains, and antifungal activity against six fungal strains (*Trichophyton longifusus*, *Candida albicans*, *Aspergillus flavus*, *Microsporum canis*, *Fusarium solani* and *Candida glabrata*). *In vitro* Brine Shrimp bioassay has also been carried out to study the cytotoxic properties of these compounds.

## Experimental

### *Materials and methods*

All chemicals used were of analar grade. All metal salts were used as chloride. Melting points were recorded on Fisher Johns melting point apparatus. Infrared spectra were recorded on SHIMADZU FT-IR spectrometer. The C, H and N analyses was carried out using a Perkin Elmer, USA model. The $^1$H and $^{13}$C NMR spectra were recorded in DMSO-$d_6$ using TMS as internal standard on a Bruker Spectrospin Avance DPX-500 spectrometer. Electron impact mass spectra (EIMS) were recorded on JEOL MS Route Instrument. *In vitro* antibacterial, antifungal and cytotoxic properties were studied at HEJ Research Institute of Chemistry, International Centre for Chemical Sciences, University of Karachi, Pakistan and Department of Chemistry, The Islamia University, of Bahawalpur, Pakistan.

### *General procedure for synthesis of triazole Schiff bases ligands* $\mathbf{L^1}$–$\mathbf{L^3}$

#### *N-[(E)-1H-pyrrol-2-ylmethylidene]-1H-1,2,4-triazol-3-amine* $\mathbf{L^1}$

Pyrrole-2-carboxaldehyde (0.95 g, 10 mmol) in methanol solution (20 ml) was added to magnetically stirred methanol solution (20 ml) of 3-amino 1,2,4 triazole (0.84 g, 10 mmol) and mixture was refluxed for 5 h through monitoring by TLC. After completion of the reaction, the resultant mixture was cooled to room temperature, filtered and reduced nearly half of its volume by rotary evaporator. It was then allowed to stay at room temperature for 3 h which resulted in the formation of a light-brown solid product. It was filtered, washed with methanol and recrystallized with a mixture of ethanol:methanol (1:1). The same procedure was used for the synthesis of ligands $\mathbf{L^2}$ and $\mathbf{L^3}$. However the ligand $\mathbf{L^3}$ was precipitated during refluxing, filtered and washed with hot methanol and recrystallized with a mixture of ethanol:methanol (1:1). The purity of product was checked by TLC.

#### *N-[(E)-1H-pyrrol-2-ylmethylidene]-1H-1,2,4-triazol-3-amine* $\mathbf{L^1}$

Yield: 76% (1.22 g). Color (light-brown). M.p. 190–192 °C. IR (KBr, cm$^{-1}$): 3185 (NH), 3120 (NH, pyrrole), 1631 (HC═N), 1610 (C═N, triazole), 1570, 1540 (C═C), 1025 (N—N). $^1$H NMR (DMSO-$d_6$, δ, ppm): 6.24 (dd, 1H, $J$ = 4.6, 4.0 Hz, pyrrole $C_4$—H), 6.86 (d, 1H, $J$ = 4.0 Hz, pyrrole $C_3$—H), 7.11 (d, 1H, $J$ = 4.6 Hz, pyrrole $C_5$—H), 8.30 (s, 1H, triazole C—H), 8.89 (s, 1H, azomethine C—H), 11.92 (s, 1H, pyrrole NH), 13.69 (s, 1H, triazole NH). $^{13}$C NMR (DMSO-$d_6$, δ, ppm): 114.5 ($C_4$), 116.6 ($C_3$), 120.7 ($C_5$), 131.5 ($C_2$), 153.7 (C triazole), 155.8 (C triazole), 159.9 (C azomethine). Anal. Calcd. for $C_7H_7N_5$ (161.16): C: 52.17; H: 4.38; N: 43.45; Found: C: 52.39; H: 4.46; N: 43.72%. Mass spectrum (ESI) $[M]^+$ = 161.16.

#### *N-[(E)-(4-bromothiophen-2-yl)methylidene]-1H-1,2,4-triazol-3-amine* $\mathbf{L^2}$

Yield: 75% (1.93 g). Color (off-white). M.p. 215–217 °C. IR (KBr, cm$^{-1}$): 3184 (NH), 1630 (HC═N), 1608 (C═N, triazole), 1570, 1545 (C═C), 1025 (N—N), 965 (C—S), 670 (C—Br). $^1$H NMR (DMSO-$d_6$, δ, ppm): 7.85 (s, 1H, thienyl $C_3$—H), 8.0 (s, 1H, thienyl $C_5$—H), 8.55 (s, 1H, triazole C—H), 9.30 (s, 1H, azomethine C—H), 14.00 (s, 1H, triazole NH). $^{13}$C NMR (DMSO-$d_6$, δ, ppm): 116.7 ($C_4$), 123.9 ($C_5$), 125.2 ($C_3$), 144.6 ($C_2$), 153.4 (C triazole), 156.2 (C triazole), 159.5 (C azomethine). Anal. Calcd. for $C_7H_5N_4SBr$ (257.11): C: 32.70; H: 1.96; N: 21.79; S: 12.47; Br: 31.08; Found: C: 33.06; H: 1.89; N: 22.10; S: 12.34; Br: 30.94%. Mass spectrum (ESI) $[M]^+$ = 257.0.

#### *4-Iodo-2-[(E)-(1H-1,2,4-triazol-3-ylimino)methyl]phenol* $\mathbf{L^3}$

Yield: 76% (2.40 g). Color (light-yellow). M.p. 255–257 °C. IR (KBr, cm$^{-1}$): 3270 (OH), 3182 (NH), 1630 (HC═N), 1610 (C═N, triazole), 1030 (N—N). $^1$H NMR (DMSO-$d_6$, δ, ppm): 6.86 (d, 1H, $J$ = 8.3 Hz, phenyl $C_6$—H), 7.7 (dd, 1H, $J$ = 8.3, 2.5 Hz, phenyl $C_5$—H), 8.19 (d, 1H, $J$ = 2.5 Hz, phenyl $C_3$—H), 8.48 (s, 1H, triazole C—H), 9.4 (s, 1H, azomethine C—H), 12.3 (s, 1H, OH), 14.1 (s, 1H, triazole NH). $^{13}$C NMR (DMSO-$d_6$, δ, ppm): 114.7 ($C_4$), 119.9 ($C_6$), 122.5 ($C_2$), 138.5 ($C_3$), 141.1 ($C_5$), 153.4 (C triazole), 156.6 (C triazole), 161.4 (C azomethine), 163.1 ($C_1$). Anal. Calcd. for $C_9H_7IN_4O$

**Table 1**
Physical measurements and analytical data of the metal(II) complexes.

| No. | Molecular mass/molecular formula | M.P (dec.) yield | | Found (calc.) % | | | |
|---|---|---|---|---|---|---|---|
| | | (°C) | (%) | **C** | **H** | N | M |
| 1 | [Co($\mathbf{L^1}$–H)$_2$] [379.2] | 239–241 | 61 | 43.99 | 3.19 | 37.25 | 15.49 |
| | $C_{14}H_{12}N_{10}Co$ | | | (44.34) | (3.19) | (36.93) | (15.54) |
| 2 | [Ni($\mathbf{L^1}$–H)$_2$] [379.0] | 248–250 | 63 | 44.09 | 3.06 | 36.60 | 15.45 |
| | $C_{14}H_{12}N_{10}Ni$ | | | (44.37) | (3.19) | (36.96) | (15.49) |
| 3 | [Cu($\mathbf{L^1}$–H)$_2$] [383.8] | 245–247 | 60 | 43.43 | 3.15 | 36.49 | 16.62 |
| | $C_{14}H_{12}N_{10}Cu$ | | | (43.81) | (3.15) | (36.49) | (16.55) |
| 4 | [Zn($\mathbf{L^1}$–H)$_2$] [385.7] | 253–255 | 59 | 43.90 | 3.02 | 36.54 | 16.95 |
| | $C_{14}H_{12}N_{10}Zn$ | | | (43.59) | (3.14) | (36.31) | (16.95) |
| 5 | [Co($\mathbf{L^2}$)$_2$]Cl$_2$ [644.06] | 245–247 | 60 | 25.84 | 1.39 | 17.19 | 9.19 |
| | $C_{14}H_{10}N_8S_2Br_2Cl_2Co$ | | | (26.11) | (1.56) | (17.40) | (9.15) |
| 6 | [Ni($\mathbf{L^2}$)$_2$]Cl$_2$ [643.81] | 251–253 | 59 | 26.37 | 1.74 | 17.57 | 9.07 |
| | $C_{14}H_{10}N_8S_2Br_2Cl_2Ni$ | | | (17.19) | (1.57) | (17.40) | (9.12) |
| 7 | [Cu($\mathbf{L^2}$)$_2$]Cl$_2$ [648.67] | 258–260 | 58 | 26.18 | 1.43 | 17.41 | 9.84 |
| | $C_{14}H_{10}N_8S_2Br_2Cl_2Cu$ | | | (25.92) | (1.55) | (17.27) | (9.80) |
| 8 | [Zn($\mathbf{L^2}$)$_2$]Cl$_2$ [650.52] | 266–268 | 59 | 26.05 | 1.61 | 17.08 | 10.08 |
| | $C_{14}H_{10}N_8S_2Br_2Cl_2Zn$ | | | (25.85) | (1.55) | (17.22) | (10.05) |
| 9 | [Co($\mathbf{L^3}$–H)$_2$] [685.08] | 279–281 | 64 | 31.34 | 1.65 | 16.45 | 8.57 |
| | $C_{18}H_{12}N_8O_2I_2Co$ | | | (31.56) | (1.77) | (16.36) | (8.60) |
| 10 | [Ni($\mathbf{L^3}$–H)$_2$] [684.84] | 274–276 | 62 | 31.60 | 1.69 | 16.48 | 8.58 |
| | $C_{18}H_{12}N_8O_2I_2Ni$ | | | (31.57) | (1.77) | (16.36) | (8.60) |
| 11 | [Cu($\mathbf{L^3}$–H)$_2$] [689.69] | 284–286 | 65 | 31.35 | 1.69 | 16.29 | 9.17 |
| | $C_{18}H_{12}N_8O_2I_2Cu$ | | | (31.35) | (1.75) | (16.25) | (9.21) |
| 12 | [Zn($\mathbf{L^3}$–H)$_2$] [691.55] | 293–295 | 63 | 31.43 | 1.84 | 16.14 | 9.18 |
| | $C_{18}H_{12}N_8O_2I_2Zn$ | | | (31.36) | (1.75) | (16.20) | (9.21) |

(314.08): C: 34.42; H: 2.25; N: 17.84; I: 40.40; Found: C: 34.24; H: 2.18; N: 18.04; I: 40.27%. Mass spectrum (ESI) $[M]^+$ = 314.0.

*General procedure for the synthesis of complexes **1**–**12***

Preparation of cobalt (II) complex with N-[(E)-1H-pyrrol-2-ylmethylidene]-1H-1,2,4-triazol-3-amine $\mathbf{L^1}$ (1).

A hot ethanol solution (20 mL) of Co(II) $Cl_2.6H_2O$ (0.952 g, 4 mmol) was added drop wise to a magnetically stirred solution of N-[(E)-1H-pyrrol-2-ylmethylidene]-1H-1,2,4-triazol-3-amine $\mathbf{L^1}$ (1.29 g, 8 mmol) in ethanol (25 mL). The resultant mixture was refluxed for 2 h. During refluxing, a solid product precipitated out which was filtered, washed with ethanol and then with diethyl ether and dried. Recrystallization from hot aqueous ethanol (1:2) gave TLC pure product. The same method was used for the preparation of other complexes (Scheme 1). Physical, analytical and spectral data is given in Tables 1 and 2.

*NMR data of Zn (II) complexes*

*[Zn ($L^1$-H)$_2$] (**4**)*

$^1$H NMR of Zn (II) complex (DMSO-$d_6$, δ, ppm): 6.36 (dd, 2H, $J$ = 4.6, 4.0 Hz, pyrrole $C_4$—H), 6.97 (d, 2H, $J$ = 4.0 Hz, pyrrole, $C_3$—H), 7.46 (d, 2H, $J$ = 4.6 Hz, pyrrole, $C_5$—H), 8.67 (s, 2H, triazole, C—H), 9.34 (s, 2H, C—H azomethine), 13.81 (s, 2H, triazole NH). $^{13}$C NMR of Zn(II) complex (DMSO-$d_6$, δ, ppm): 114.9 ($C_4$), 116.95 ($C_3$), 121.96 ($C_5$), 132.70 ($C_2$), 154.86 (C triazole), 157.37 (C triazole), 161.6 (C azomethine).

*[Zn ($\mathbf{L^2}$)$_2$] (**8**)*

$^1$H NMR of Zn (II) complex (DMSO-$d_6$, δ, ppm): 7.97 (d, 2H, $J$ = 3.5 Hz, furanyl $C_3$—H), 8.35 (d, 2H, $J$ = 3.5 Hz, furanyl $C_5$—H), 8.89 (s, 2H, triazole C—H), 9.69 (s, 2H, C—H azomethine), 14.10 (s, 2H, triazole NH). $^{13}$C NMR of Zn(II) complex (DMSO-$d_6$, δ, ppm): 116.89 ($C_4$), 125.27 ($C_5$), 125.44 ($C_3$), 145.7 ($C_2$), 154.73 (Ctriazole), 157.94 (C triazole), 161.2 (C azomethine).

*[Zn ($\mathbf{L^3}$-H)$_2$] (**12**)*

$^1$H NMR of Zn (II) complex (DMSO-$d_6$, δ, ppm): 7.02 (d, 2H, $J$ = 8.3 Hz, phenyl $C_6$—H), 7.86 (dd, 2H, $J$ = 8.3, 2.5 Hz, phenyl $C_5$—H), 8.33 (d, 2H, $J$ = 2.5 Hz, phenyl $C_3$—H), 8.81 (s, 2H, triazole C—H), 9.81 (s, 2H, C—H azomethine), 14.13 (s, 2H, triazole NH); $^{13}$C NMR of Zn(II) complex (DMSO-$d_6$, δ, ppm): 115.1 ($C_4$), 120.32 ($C_6$), 122.78 ($C_2$), 138.86 ($C_3$), 141.4 ($C_5$), 154.72 (C triazole), 158.30 (Ctriazole), 162.59 (C azomethine), 164.25 ($C_1$).

## Biological activity

*Antibacterial studies*

The entire newly synthesized Schiff base $\mathbf{L^1}$–$\mathbf{L^3}$ and their respective metal(II) complexes **1**–**12** were tested against four Gram-negative (*E. coli*, *S. sonnei*, *P. aeruginosa*, *S. typhi*) and two Gram-positive (*S. aureus*, *B. subtilis*) bacterial strains by the disk diffusion method [21]. The test compounds (ligand/complex) were dissolved in DMSO to get 10 mg/mL solution. A known volume (10 μL) of the solution was applied with the help of a micropipette onto the sterilized filter paper disks. The disks were dried at room temperature overnight and stored in sterilized dry containers. Disks soaked with 10 μL of DMSO and dried in air at room temperature were used as the negative control. The standard antibiotic disks used as positive control were prepared as mention above in the laboratory by applying a known concentration of the standard antibiotic solution. Ampicillin was used as standard antibiotic. Bacterial culture was grown in nutrient broth medium at 37 °C overnight and spread onto solidified nutrient agar medium in Petri plates using sterilized cotton swabs. Test and control disks were then applied to the medium surface with the help of sterilized forceps. The plates were incubated at 37 °C for 24–48 h. The results were recorded by measuring the zone of inhibition in mm against each compound. The experiments were carried out in triplicate and the values obtained were statistically analyzed.

*Antifungal activity (in vitro)*

Antifungal activities of all compounds were studied against six fungal strains (*T. longifusus*, *C. albicans*, *A. flavus*, *M. canis*, *F. solani* and *C. glabrata)* according to literature protocol [18]. Sabouraud dextrose agar (Oxoid, Hampshire, England) was seeded with $10^5$ (cfu) mL$^{-1}$ fungal spore suspensions and transferred to petri

**Table 2**
Conductivity, magnetic and spectral data of metal(II) complexes.

| No. $\Omega^{-1}$ cm$^2$ mol$^{-1}$ | $\Omega_M$ | B.M ($\mu_{eff}$) | $\lambda_{max}$ (cm$^{-1}$) | IR (cm$^{-1}$) |
|---|---|---|---|---|
| **1** | 14.4 | 4.34 | 8892, 17,759, 30,150 | 3185 (NH), 1618 (HC=N), 1594 (C=N), 1025 (N—N), 540 (M—N), 520 (M—N) |
| **2** | 18.7 | 3.47 | 10,085, 16,105, 29,635 | 3185 (NH), 1617 (HC=N), 1597 (C=N), 1025 (N—N), 545 (M—N), 525 (M—N) |
| **3** | 15.8 | 1.57 | 14,876, 25,800 | 3185 (NH), 1616 (HC=N), 1596 (C=N), 1025 (N—N), 540 (M—N), 523 (M—N), |
| **4** | 17.5 | Dia | 28,778 | 3185 (NH), 1616 (HC=N), 1598 (C=N), 1025 (N—N), 535 (M—N), 520 (M—N) |
| **5** | 87.6 | 4.62 | 8786, 17,334, 29,889 | 3184 (NH), 1615 (HC=N), 1591 (C=N), 1025 (N—N), 945 (C—S), 670 (C—Br), 520 (M—N), 462 (M—S) |
| **6** | 88.4 | 3.41 | 10,180, 16,775, 29,440 | 3184 (NH), 1614 (HC=N), 1594 (C=N), 1025 (N—N), 948 (C—S), 670 (C—Br), 525 (M—N), 465 (M—S) |
| **7** | 85.0 | 1.51 | 14,975, 25,267 | 3184 (NH), 1617 (HC=N), 1592 (C=N), 1025 (N—N), 945 (C—S), 670 (C—Br), 521 (M—N), 460 (M—S) |
| **8** | 89.5 | Dia | 28,763 | 3184 (NH), 1616 (HC=N), 1596 (C=N), 1025 (N—N), 950 (C—S), 670 (C—Br), 529 (M—N), 466 (M—S) |
| **9** | 11.5 | 4.44 | 8823, 17,677, 29,726 | 3182 (NH), 1618 (HC=N), 1595 (C=N), 1380 (C—O), 1030 (N—N), 532 (M—N), 462 (M—O) |
| **10** | 13.7 | 3.27 | 10,156, 16,075, 29,210 | 3182 (NH), 1618 (HC=N), 1595 (C=N), 1380 (C—O), 1030 (N—N), 526 (M—N), 452 (M—O) |
| **11** | 18.2 | 1.67 | 14,822, 25,717 | 3182 (NH), 1615 (HC=N), 1598 (C=N), 1384 (C—O), 1030 (N—N), 528 (M—N), 459 (M—O) |
| **12** | 11.6 | Dia | 28,749 | 3182 (NH), 1616 (HC=N), 1596 (C=N), 1390 (C—O), 1030 (N—N), 524 (M—N), 456 (M—O) |

plates. Disks soaked in 20 ml (200 μg/mL in DMSO) of test compounds were placed at different positions on the agar surface. The plates were incubated at 32 °C for 7 days. The results were recorded as % of inhibition and compared with standard drugs miconazole and amphotericin B [22].

*Minimum inhibitory concentration (MIC)*

Compounds containing significant antibacterial activity (over 80%) were selected for minimum inhibitory concentration (MIC) studies. The minimum inhibitory concentration was determined using the disk diffusion technique by preparing disks containing 10, 25, 50 and 100 μg/mL of the test compounds and applying the protocol.

*In vitro Cytotoxicity*

*In vitro* cytotoxic activity of all synthesized ligands **L$^1$**–**L$^3$** and their metal(II) complexes **1**–**12** were studied using the protocol of Meyer et al. Brine shrimp (Artemia salina leach) eggs were hatched in a shallow rectangular plastic dish (22 × 32 cm), filled with artificial seawater, which was prepared with commercial salt mixture and double distilled water [20]. An unequal partition was made in the plastic dish with the help of a perforated device. Approximately 50 mg of eggs were sprinkled into the large compartment, in dark while the matter compartment was opened to ordinary light. After 2 days nauplii were collected by a pipette from the side in ordinary light. A sample of the test compound was prepared by dissolving 20 mg of each compound in 2 mL of DMSO. From this stock solutions 500, 50 and 5 μg/mL were transferred to 9 vials (three for each dilutions were used for each test sample and $Ld_{60}$ is the mean of three values) and one vial was kept as control having 2 mL of DMSO only for determine its any participating role. The solvent was allowed to evaporate overnight. After 2 days, when shrimp larvae were ready, sea water (1 mL) and 10 shrimps were added to each vial (30 shrimps/dilution) and the volume was adjusted with sea water to 5 mL per vial. After 24 h the number of survivors was counted. Data were analyzed by Finney computer program to determine the $LD_{50}$ values [23].

## Results and discussion

*Chemistry*

The Schiff base ligands **L$^1$**–**L$^3$** were prepared by the condensation reaction of 3-amino1*H*-1,2,4-triazole with a 1*H*-pyrrole-2-carboxaldehyde, 4-bromo-thiophene-2-carboxaldehyde and 5-iodo-2-hydroxybenzaldehydes, respectively, under reflux as shown in Scheme 1. All the synthesized derivatives of triazole were soluble in ethanol, dioxane, DMF and DMSO at room temperature and in methanol on heating only. The composition of ligands was consistent with their micro-analytical and mass spectral data. The metal complexes **1**–**12** of these ligands were prepared by the reaction of corresponding ligands with metal (Co(II), Ni(II), Cu(II) and Zn(II)) as chlorides in a (1:2) (metal:ligand) molar ratio. All the metal complexes were air and moisture stable at room temperature. They were insoluble in common organic solvents and only soluble in DMF and DMSO. Physical measurements and analytical data of the complexes **1**–**12** are given in Tables 1 and 2.

*IR spectra*

The characteristic bands of IR spectra of ligands **L$^1$**–**L$^3$** and their metal(II) complexes are reported in experimental section and in Table 2. All the ligands possessed potential donor sites like azomethine linkage (—C=N), triazole ring nitrogen (—C=N), hydroxyl (—OH), thienyl (—C—S) and pyrrole (N—H) groups which have tendency to coordinate with the metal ions. The IR spectra of all the ligands showed [21–23] the peaks at 3182–3185, 1608–1610 and 1025–1030 cm$^{-1}$ respectively due to vibration of (N—H), (C=N) and (N—N) of triazole moiety. Originally, 3-amino-1,2,4-triazole and aldehydes showed peaks at 3325 and 1715 cm$^{-1}$ respectively, due to aldehydic (CHO) and amino ($NH_2$) group vibrations. In the spectra of the ligands **L$^1$**–**L$^3$**, the peaks at 1715 and 3325 cm$^{-1}$ due to aldehydic (CHO) and amino ($NH_2$) groups of the original moieties are completely disappeared and in turn, a new sharp band appeared at 1630–1631 cm$^{-1}$ assigned to the azomethine (—C=N) linkage [23]. The spectrum of ligand **L$^1$** showed peak at 3120 cm$^{-1}$ assigned [22] the (NH) group of pyrrole ring. Similarly, the ligand

**L²** showed bands at 965 and 670 $cm^{-1}$ assigned [23] the thienyl (C—S) and (C—Br) groups. Moreover, the ligand **L³** showed broad spectral band at 3270 $cm^{-1}$ due to vibrations of intramolecular hydrogen bonded [22] hydroxyl (—OH) group with azomethine (—C=N) group. The comparison of the IR spectra of Schiff base ligands with corresponding metal complexes gave clue the different modes of absorption in complexation of ligands with the metal ions. All the Schiff base ligands showing IR spectral bands at 1630–1631 $cm^{-1}$ due to azomethine-N shifted to lower frequency (13–17 $cm^{-1}$) at 1614–1618 $cm^{-1}$ representing the involvement of the azomethine-N in the complex formation. Similarly, the triazole ring (C=N) band originally appearing at 1608–1610 $cm^{-1}$ in the spectra of the ligands shifted to lower frequency at 1591–1598 $cm^{-1}$ in spectra of metal complexes by 12–19 $cm^{-1}$ indicative [25] of the coordination of triazole ring nitrogen in the complexes. The overall conclusions drawn from the comparison of the spectra of the metal(II) complexes with the ligands are as below

1. In all the metal(II) complexes, a new band appeared [26] at 520–532 $cm^{-1}$ due to $\nu$(M–N) vibrations indicating the coordination of nitrogen of triazole ring with the metal ions. However, the band appearing at 1025–1030 $cm^{-1}$ in triazole ring assigned to $\nu$(N–N) mode remained unchanged in the spectra of all the metal(II) complexes thus indicating the non-involvement of nitrogen of (N-N) of triazole ring.
2. The IR spectra of ligand, **L¹** showed a band at 3120 $cm^{-1}$ due to NH vibrations, this band disappeared in spectra of their metal(II) complexes, **1**–**4** due to the deprotonation of the NH moiety during coordination. The appearance of a weak band at 535–545 $cm^{-1}$ due to $\nu$(M–N) vibrations, further supported the evidence of the metal–nitrogen (M–N) linkage.
3. The disappearance [25] of broad band of $\nu$(OH) at 3270 $cm^{-1}$ in spectra of metal complexes **9**–**12** and in turn appearance of new band assigned to (C—O) at 1380–1390 $cm^{-1}$ revealed deprotonation and coordination of hydroxyl-O to the metal atom. The coordination of metal to oxygen is further justified by the appearance of a new band at 452–462 $cm^{-1}$ due to M—O.
4. The bands appearing at 965 $cm^{-1}$ in the spectra of the ligands, **L²** due to (C—S) vibration is shifted to lower frequency at 945–950 $cm^{-1}$ by 15–20 $cm^{-1}$ in the spectra of the metal(II) complexes, **5**–**8** indicating participation and coordination of thienyl-S ring in the complexation phenomenon. This coordination is further justified by the appearance [25] of new band at 460–466 $cm^{-1}$ due to M–S.
5. All other bands remain unchanged in the spectra of all ligands and their corresponding metal complexes.
6. The IR spectra of all ligands and their metal(II) complexes conclusively shown that all the ligands are coordinated to the metal atoms tri-dentately *via* the azomethine-N, triazole-N, thiophene-S/pyrrolyl-N or hydroxyl-O groups.

*$^1$H NMR spectra*

The $^1$H NMR spectral data of the ligands **L¹**–**L³** and their diamagnetic Zn(II) complexes are recorded in the experimental part. The appeared signals of all the protons of Schiff bases ligands and Zn(II) complexes due to heteroaromatic/aromatic groups were found [26] as to be in their expected region. The spectra of all the ligands **L¹**–**L³** displayed [27] azomethine (—C**H**=N) and triazole C—**H** protons as a singlet at 8.89–9.40 and 8.30–8.55 ppm respectively. The peaks appearing in the spectrum of ligand **L¹** at 6.86–7.11 ppm were assigned to $C_3$—**H** and $C_5$—**H** protons as a doublet and at 6.24 ppm were assigned to $C_4$—**H** as double of the doublet. The spectrum of ligand **L¹** also displayed a peak of pyrrole-N**H** proton at 11.92 ppm. The Schiff base ligand **L²** exhibited $C_3$—**H** and $C_5$—**H** protons as singlet at 7.85 and 8.0 ppm. The ligand **L³** displayed [28] proton of hydroxyl group (—O**H**) as a singlet at 12.3 ppm. The strong experienced down field shifting of hydroxyl proton indicated [29] its participation in intramolecular hydrogen bonding with the azomethine group. The ligand **L³** displayed $C_3$—**H** and $C_6$—**H** protons of phenyl group as doublet at 8.19 and 6.86 ppm respectively and the same ligands showed $C_5$—**H** proton of phenyl as double of the doublet at 7.7 ppm. A broad singlet was displayed [26] at 13.69–14.1 ppm due to the N**H** proton of triazole in all the ligands observing tautomerism. The coordination of the azomethine (CH=N) and (C=N) of triazole nitrogen are assigned [27] by the downfield shifting of azomethine (—C**H**=N) and triazole (C—**H**) protons signals present at 8.89–9.40 and 8.30–8.55 ppm in the free ligands to 9.34–9.81 and 8.67–8.81 ppm in the spectra of their zinc(II) complexes, respectively. Furthermore, signal of pyrrole (N**H**), and hydroxyl (O**H**) protons appearing at 11.92 and 12.30 ppm in the spectra of ligands, **L¹** and **L³** respectively, disappeared in spectra of their corresponding zinc complexes indicating deprotonation and coordination of the nitrogen and oxygen with the zinc metal atom. The coordination of thienyl-S was justified by the downfield shifting of $C_5$—**H** proton of ligand **L²** downfield from 8.0 to 8.35 ppm in their Zn(II) complexes due to deshielding effect. All other protons overall underwent downfield shift by 0.11–0.25 ppm due to the increased conjugation [29] in the spectra of the Zn(II) complexes.

*$^{13}$C NMR spectra*

The $^{13}$C NMR spectra of the Schiff base ligands **L¹**–**L³** and their Zn(II) complexes were taken in DMSO-$d_6$. The $^{13}$C NMR spectral information are reported along with their possible assignments in the experimental section and all the carbons were found in the expected region [25–28]. The $^{13}$C NMR spectra of all the Schiff base ligands **L¹**–**L³** displayed [26] the azomethine carbon (—**C**H=N) at 159.5–161.4. The spectra of ligands **L¹** and **L²** displayed [25] pyrrole and thienyl carbons in the region at 114.5–131.5 and 116.7–144.6 ppm respectively. All carbons of phenyl group in ligand **L³** appeared [26] at 114.7–163.1 ppm. The carbon $\mathbf{C}_1$ in this ligand **L³** was observed downfield at 163.1 ppm due to attachment of hydroxyl (OH) group at the same position. However the carbon **($C_4$)** of ligand **L³** was observed upfield at 114.7 ppm due to attachment of lesser electronegative iodo group. All the Schiff base ligands **L¹**–**L³** displayed [27] the triazole carbon at 153.4–156.6 ppm. The conclusion obtained from these studies provided further support to the mode of bonding explained in the IR and $^1$H NMR spectral data. The spectra of Zn(II) complexes of all Schiff base ligands exhibited [28] downfield shifting of azomethine carbon (—**C**H=N—) and triazole carbon (**C**=N) from 159.5 to 161.4 and 153.4 to 156.6 ppm in the spectra of ligands to 161.2–162.59 and 154.72–158.30 ppm in the spectra of their zinc(II) complexes respectively, indicating the coordination of azomethine and triazole nitrogen to the zinc metal ion. Similarly, the phenyl carbon **($C_1$)** of ligand **L³** existing near the coordination sites (C1—O—M) showed [28] downfield shift from 163.1 ppm in the spectra of free ligands to 164.25 ppm in the spectra of the zinc(II) complexes. In the same way, the spectra of Zn(II) complexes of ligands **L¹** and **L²** exhibited downfield shifting by 0.8–1.7 ppm in all the carbons which were attached with hetero atom like sulpher and nitrogen of thienyl and pyrrole respectively. All other carbons of the ligands in the spectra of the Zn(II) complexes underwent downfield shifting by 0.24–0.8 ppm due to the increased conjugation [29] and coordination with the metal atoms.

*Mass spectra*

The mass spectral data and fragmentation pattern of all the Schiff base ligands **L¹**–**L³** clearly justify [30,31] the formation of the ligands possessing proposed structures and their bonding pattern. The spectra of ligand **L¹** showed molecular ion peak $m/z$ 161

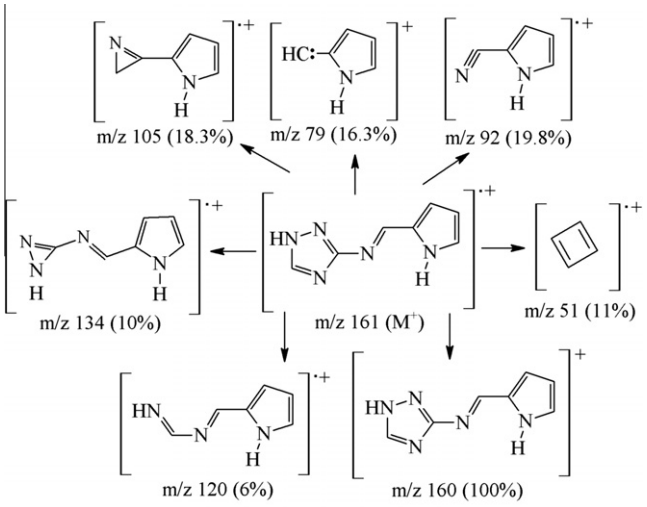


**Fig. 1.** Proposed mass fragmentation pattern of $\mathbf{L^1}$.

**Table 3**
Antibacterial bioassay (concentration used 1 mg/mL of DMSO) of ligands and metal(II) complexes.

| Compounds | Zone of inhibition (mm) | | | | | | SA | Average |
|---|---|---|---|---|---|---|---|---|
| | Gram-negative | | | Gram-positive | | | | |
| | **(a)** | **(b)** | **(c)** | **(d)** | **(e)** | **(f)** | | |
| $\mathbf{L^1}$ | 14 | 16 | 15 | 14 | 12 | 13 | 1.41 | 14.0 |
| $\mathbf{L^2}$ | 14 | 12 | 14 | 15 | 14 | 13 | 1.03 | 13.7 |
| $\mathbf{L^3}$ | 14 | 13 | 15 | 13 | 14 | 13 | 0.82 | 13.7 |
| **1** | 18 | 20 | 20 | 17 | 14 | 16 | 2.34 | 17.5 |
| **2** | 18 | 17 | 19 | 16 | 16 | 17 | 1.17 | 17.1 |
| **3** | 17 | 18 | 18 | 17 | 14 | 17 | 1.47 | 16.8 |
| **4** | 19 | 20 | 21 | 16 | 16 | 14 | 2.73 | 17.7 |
| **5** | 19 | 13 | 17 | 19 | 17 | 19 | 2.34 | 17.7 |
| **6** | 16 | 17 | 18 | 17 | 19 | 24 | 2.88 | 18.5 |
| **7** | 17 | 16 | 15 | 17 | 18 | 19 | 1.41 | 17.0 |
| **8** | 18 | 17 | 17 | 19 | 16 | 19 | 1.21 | 17.7 |
| **9** | 18 | 17 | 19 | 18 | 19 | 15 | 1.50 | 17.7 |
| **10** | 16 | 18 | 18 | 17 | 19 | 17 | 1.05 | 17.5 |
| **11** | 17 | 16 | 20 | 19 | 16 | 16 | 1.75 | 17.3 |
| **12** | 16 | 17 | 18 | 17 | 18 | 16 | 0.89 | 17.0 |
| **A** | 08 | 11 | 13 | 10 | 10 | 10 | 1.63 | 10.3 |
| **SD** | 26 | 24 | 32 | 28 | 27 | 29 | 2.73 | 27.7 |

Average of ligands $\mathbf{L^1}$–$\mathbf{L^3}$ = 13.8 mm; average of complexes **1**–**12** = 17.45 mm; **(a)** = *E. coli* **(b)** = *S. sonnei* **(c)** = *P. aeruginosa* **(d)** = *S. typhi* **(e)** = *S. aureus* **(f)** = *B. subtilis*. Activity < 10 = weak; >10 = moderate; > 16 = significant: **A** = 3-amino-1*H*-1,2,4-triazole and SD = standard drug (ampicillin). SA = Statistical analysis.

(Calcd. 161.16) of $[C_7H_7N_5]^{\cdot+}$ which loses a hydrogen (H) as radical to give most stable fragment at *m*/*z* 160 of $[C_7H_6N_5]^+$. The molecular mass of ligand, $\mathbf{L^2}$ $C_7H_5N_4SBr$ was found as 257 (Calcd. 257.11) and its base peak $[C_7H_5N_4S]^+$ was observed at *m*/*z* 177. The molecular ion peak of ligand $\mathbf{L^3}$ was found as 313.9 (Calcd. 314.08) of $[C_9H_7N_4OI]^{\cdot+}$ and its most stable fragment $[C_9H_6IN_4]^+$ was observed at *m*/*z* 297. The fragmentation pattern followed the cleavage of C=N (exocyclic as well as endocyclic), C—I, C—O, C—C and C—N bonds. Fragmentation pattern of ligand $\mathbf{L^1}$ is shown as Fig. 1 in supplementary material.

### *Conductance and magnetic susceptibility measurements*

The molar conductance values of all the metal(II) complexes were obtained in DMF as a solvent at room temperature and their results in ($\Omega^{-1}$ cm$^2$ mol$^{-1}$) are recorded as in Table 2. Generally, higher molar conductance values are indicative of the electrolytic nature of the metal(II) complexes and lower values as non-electrolytic nature [32]. The molar conductance values of the metal complexes **5**–**8** fall in the range 85.0–89.5 $\Omega^{-1}$ cm$^2$ mol$^{-1}$ assigned to their electrolytic nature. However, the molar conductance data of the metal complexes **1**–**4** and **9**–**12** showed their molar conductance values in the range 11.5–18.7 $\Omega^{-1}$ cm$^2$ mol$^{-1}$ indicative of their non-electrolytic nature [32]. The determine magnetic moment (B.M) values of all the metal(II) complexes, **1**–**12** at room temperature were recorded in Table 2. The magnetic moment values of Co(II) complexes were found in the range of 4.34–4.62 B.M suggesting the Co(II) complexes as high-spin with three unpaired electrons in an octahedral [33] environment. The Ni(II) complexes exhibited magnetic moment values in the range of 3.27–3.47 B.M representative of two unpaired electrons per Ni(II) ion suggesting these complexes to have octahedral [34] geometry. The obtained magnetic moment values 1.51–1.67 B.M for Cu(II) complexes are indicative of one unpaired electron per Cu(II) ion for $d_9$-system suggesting spin-free distorted octahedral geometry. All the Zn(II) complexes were found to be diamagnetic [35] as expected .

### *Electronic spectra*

The electronic spectral values of Co(II), Ni(II), Cu(II) and Zn(II) complexes **1**–**12** are recorded in Table 2. The electronic spectra of Co(II) complexes generally showed three absorption bands in the region at 8786–8892, 17,334–17,759 and 29,726–30,150 cm$^{-1}$ which assigned to transitions $^4T_{1g} \rightarrow {}^4T_{2g}(F)$, $^4T_{1g} \rightarrow {}^4A_{2g}(F)$ and $^4T_{1g} \rightarrow {}^4T_g(P)$, showing an octahedral geometry [36] around the Co(II) ion. The electronic spectral data of Ni(II) complexes showed d-d bands in the region 10,085–10,180, 16,075–16,775 and 29,210–29,635 cm$^{-1}$ respectively, to assigned the transitions $^3A_{2g}(F) \rightarrow {}^3T_{2g}(F)$, $^3A_{2g}(F) \rightarrow {}^3T_{1g}(F)$ and $^3A_{2g}(F) \rightarrow {}^3T_{2g}(F)$, which are characteristic of Ni(II) in octahedral geometry . The electronic spectra of Cu(II) complexes exhibited low-energy absorption band at 14,822–14,975 cm$^{-1}$ assigned to the transitions $^2E_g \rightarrow {}^2T_{2g}$. The high-energy band at 25,267–25,800 cm$^{-1}$ is due to forbidden ligand → metal charge transfer. On the basis of which a distorted octahedral geometry is suggested for Cu(II) complexes [37]. The diamagnetic Zn(II) complexes did not show any *d*–*d* transitions and their spectra were dominated [36] only by the charge transfer band at 28,749–28,778 cm$^{-1}$.

## Biological activity

### *Antibacterial bioassay*

The antibacterial activity of Schiff base ligands, $\mathbf{L^1}$–$\mathbf{L^3}$ and their metal(II) complexes, **1**–**12** were studied against four Gram-negative (*E. coli*, *S. sonnei*, *P. aeruginosa*, *S. typhi*) and two Gram-positive (*S. aureus*, *B. subtilis*) bacterial strains according to the literature protocol and their results were recorded in Table 3. The obtained results were compared with standard drug, ampicillin and simple triazole moiety, 3-amino-1*H*-1,2,4-triazole (Fig. 2). The Schiff base ligands $\mathbf{L^1}$–$\mathbf{L^3}$ exhibited varying degree of inhibitory effects on the growth of different tested strains and their metal(II) complexes showed moderate to significant inhibitory effects on the growth of different tested bacterial strains. The antibacterial activity data of Schiff base ligand $\mathbf{L^1}$ showed significant activity (66%) against **(b)** and moderate activity (44–50%) against **(a)** and **(c)**–**(f)** bacterial strains. The Schiff base ligands, $\mathbf{L^2}$ and $\mathbf{L^3}$ showed moderate activity (43–53%) against all the tested bacterial strains. The activity data of metal(II) complexes exhibited that the complexes **2**, **6**, **8**, **10**, **11** and **12** showed significant activity (54–82%) against all the tested bacterial strains, while the complexes **4** and **9** showed significant

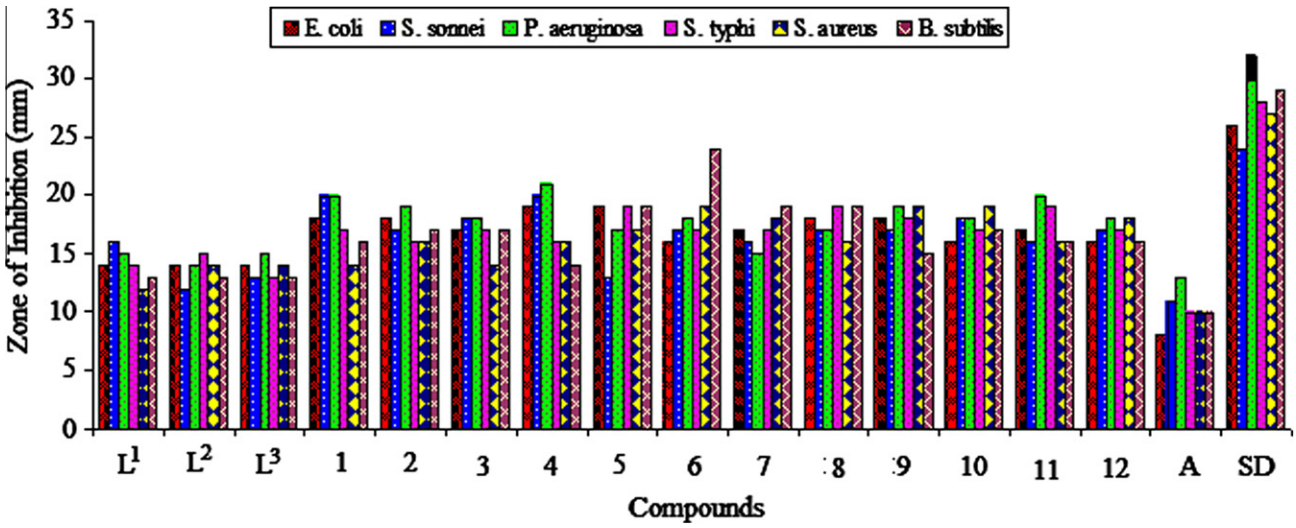


**Fig. 2.** Comparison of antibacterial activity.

**Table 4**
Antifungal bioassay (concentration used 200 μg/mL) of ligands and metal(II) complexes.

| Compounds | % Inhibition (mm) | | | | | | SA | Average |
|---|---|---|---|---|---|---|---|---|
| | **(a)** | **(b)** | **(c)** | **(d)** | **(e)** | **(f)** | | |
| **$L^1$** | 39 | 55 | 23 | 49 | 43 | 61 | 13.38 | 46.2 |
| **$L^2$** | 28 | 43 | 59 | 41 | 34 | 56 | 12.11 | 43.5 |
| **$L^3$** | 34 | 62 | 43 | 52 | 25 | 44 | 13.02 | 43.3 |
| **1** | 43 | 57 | 29 | 55 | 47 | 67 | 13.12 | 49.7 |
| **2** | 38 | 58 | 21 | 50 | 45 | 73 | 17.69 | 47.5 |
| **3** | 44 | 60 | 25 | 52 | 46 | 64 | 13.88 | 48.7 |
| **4** | 40 | 55 | 29 | 60 | 45 | 62 | 12.81 | 48.5 |
| **5** | 41 | 46 | 54 | 43 | 34 | 61 | 10.04 | 46.0 |
| **6** | 39 | 45 | 55 | 50 | 35 | 61 | 8.86 | 47.5 |
| **7** | 34 | 44 | 54 | 42 | 40 | 54 | 10.99 | 44.3 |
| **8** | 31 | 48 | 59 | 39 | 38 | 62 | 12.38 | 44.3 |
| **9** | 39 | 65 | 44 | 57 | 28 | 49 | 13.13 | 47.0 |
| **10** | 36 | 69 | 39 | 61 | 26 | 46 | 16.14 | 46.2 |
| **11** | 38 | 65 | 46 | 56 | 31 | 44 | 12.26 | 46.7 |
| **12** | 45 | 67 | 48 | 54 | 24 | 53 | 14.11 | 48.3 |
| **SD** | A | B | C | D | E | F | | |

Average of activity ligands **$L^1$–$L^3$** = 44.33%; average activity of complexes **1–12** = 47.06%. **(a)** = *T. longifucus* **(b)** = *C. albicans* **(c)** = *A. flavus* **(d)** = *M. canis* **(e)** = *F. Solani* **(f)** = *C. glabrata*, **SD** = standard drugs MIC μg/mL; A = miconazole (70 μg/mL:1.6822 × $10^{-7}$ M/mL), B = miconazole (110.8 μg/mL:2.6626 × $10^{-7}$ M/mL), C = amphotericin B (20 μg/mL:2.1642 × $10^{-8}$ M/mL), D = miconazole (98.4 μg/mL:2.3647 × $10^{-7}$ M/mL), E = miconazole (73.25 μg/mL: 1.7603 × $10^{-7}$ M/mL), F = miconazole (110.8 μg/mL: 2.66266 × $10^{-7}$ M/mL). **SA** = Statistical analysis.

activity (57–83%) against **(a)–(e)**, and moderate activity (48–52%) against **(f)** bacterial strains. Similarly, the metal(II) complexes, **1** and **3** showed significant activity (55–83%) against **(a)–(d)** and **(f)** and moderate activity (52%) against **(e)** bacterial strains. The complex **5** possessed significant activity (54–73%) against **(a)** and **(c)–(f)** and moderate activity (52%) against **(b)** bacterial strains. In the same way, the metal(II) complex **7** also showed significant activity (61–66%) against **(a)**, **(b)** and **(d)–(f)** and moderate activity (46%) against **(c)** bacterial strains. The comparison of the average activity value (13.8 mm) of Schiff base ligands and the average activity value (17.45 mm) of their corresponding metal(II) complexes revealed [37,38] that the activity of the metal(II) complexes is increased upon coordination with metal ions.

*Antifungal bioassay*

The Schiff base ligands **$L^1$–$L^3$** and their metal(II) complexes, **1–12** were studied against, *T. longifusus*, *Candida albican*, *A. flavus*, *M. canis*, *F. solani* and *C. glabrata* fungal strains and their results recorded in Table 4. The obtained results were compared with the standard drugs miconazole and amphotericin B. The ligand **$L^1$** showed significant activity (55–61%) against **(b)** and **(f)** and moderate activity (39–49%) against **(a)**, **(d)** and **(e)** and weak activity against **(c)** fungal strains. However, the same ligand showed weak activity (23%) against **(c)** fungal strain. Similarly, the ligand, **$L^2$** possessed significant activity (56–59%) against **(c)** and **(f)**, and moderate activity (34–43%) against **(b)**, **(d)** and **(e)** and weaker activity (28%) against **(a)** fungal strains. The ligand **$L^3$** alsoshowed significant activity (62%) against **(b)** and moderate activity (34–52%) against **(a)**, **(c)**, **(d)** and **(f)** and weaker activity (25%) against **(e)** fungal strains. From the antifungal activity data it was observed that the metal(II) complexes, **1–4** possessed significant activity (55–73%) against **(b)** and **(f)** and moderate activity (38–47%) against **(a)** and **(e)** and weaker activity (21–29%) against **(c)** fungal strains. The complexes, **1** and **4** also showed significant activity (55–60%) and complexes, **2** and **3** possessed moderate activity (50–52%) against fungal strain **(b)**. It was also observed that the metal complexes, **5–8** showed significant activity (54–62%) against **(c)** and **(f)** and moderate activity (34–50%) against **(a)**, **(b)**, **(d)** and **(e)** fungal strains. However, only the complex **8** showed weaker activity (31%) against **(a)** fungal strain. Similarly, the metal complexes, **9–12** showed significant activity (54–69%) against **(b)** and **(d)**, moderate (36–53%) against **(a)**, **(c)** and **(f)** and weaker activity (28–31%) against **(e)** fungal strains. Furthermore, the comparative studies of average activity value of Schiff base ligands (44.33%) and the average activity value of their metal(II) complexes (47.06%) exhibited [39] that the antifungal activity of the metal(II) complexes is increased upon coordination with metal ions. The comparative activity data of the Schiff base ligands and their metal(II) complexes is presented in Fig. 3.

*Minimum inhibitory concentration (MIC)*

The preliminary screening results of all the synthesized compounds showed that the metal complexes **1** and **6** were found to be the most active (above 80%) compounds. Therefore, these two compounds were selected for minimum inhibitory concentration (MIC) studies (Table 5). The MIC values of these compounds **1** and **6** fall in the range 1.18 × $10^{-7}$ to 1.82 × $10^{-7}$ M. The MIC results showed that the compound **6** is the most active showing maximum inhibition 1.18 × $10^{-8}$ M against bacterial strain *B. Subtilis*.

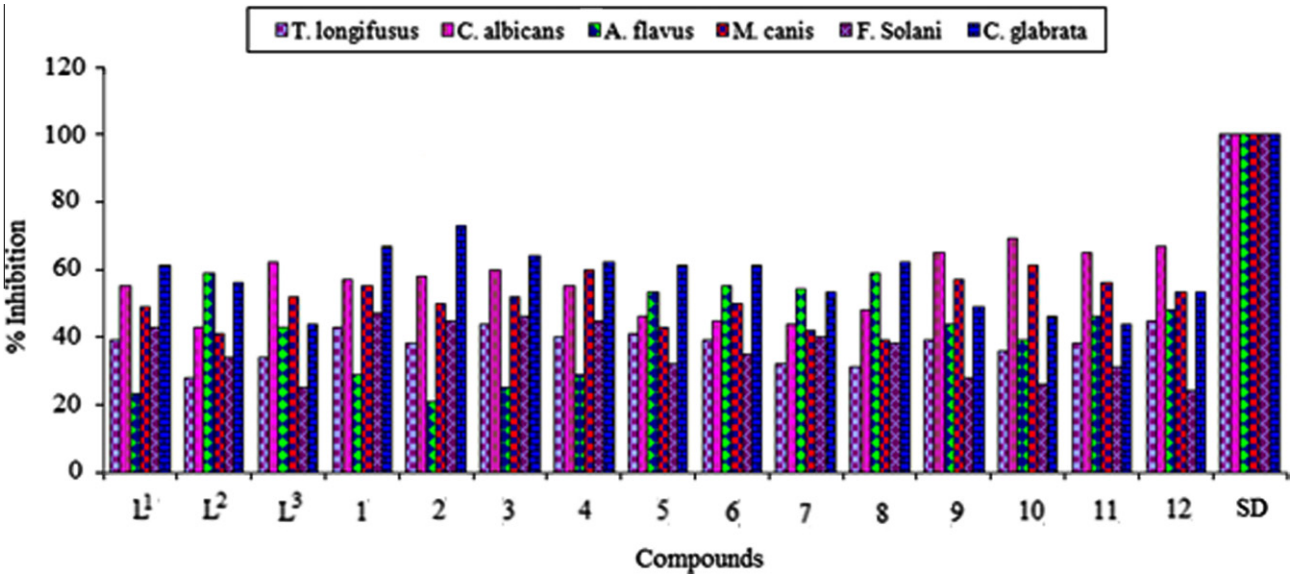


**Fig. 3.** Comparison of antifungal activity.

**Table 5**
Minimum inhibitory concentration (M/mL) of the selected compounds **1**, and **6** against selected bacteria.

| Bacterial strains | **1** | **6** |
|---|---|---|
| Gram-negative<br>*S. sonnei* | $1.82 \times 10^{-7}$ | – |
| Gram-positive<br>*B. subtilis* | – | $1.18 \times 10^{-7}$ |

**Table 6**
Brine shrimp bioassay data of the ligands **L1**–**L$^3$** and their metal(II) complexes **1**–**12**.

| Compounds | $LD_{50}$ (M/mL) | Compounds | $LD_{50}$ (M/mL) |
|---|---|---|---|
| **L$^1$** | $>1.48 \times 10^{-3}$ | **6** | $>5.45 \times 10^{-4}$ |
| **L$^2$** | $>1.54 \times 10^{-3}$ | **7** | $>5.80 \times 10^{-4}$ |
| **L$^3$** | $>8.24 \times 10^{-4}$ | **8** | $>5.33 \times 10^{-4}$ |
| **1** | $>2.64 \times 10^{-3}$ | **9** | $>7.88 \times 10^{-4}$ |
| **2** | $>9.54 \times 10^{-4}$ | **10** | $>8.18 \times 10^{-4}$ |
| **3** | $>9.66 \times 10^{-4}$ | **11** | $>6.63 \times 10^{-4}$ |
| **4** | $>1.15 \times 10^{-3}$ | **12** | $>8.55 \times 10^{-4}$ |
| **5** | $>5.39 \times 10^{-4}$ | | |

*Cytotoxic bioassay*

The synthesized ligands **L$^1$**–**L$^3$** and their metal complexes **1**–**12** were screened for their cytotoxicity (Brine Shrimp bioassay) using the protocol of Meyer et al. [24]. The cytotoxic data recorded in Table 6 revealed that all compounds were considered as almost inactive in this assay. It was interesting to note that the metal complexes showed potent cytotoxicity as compared to the ligands. This activity relationship may serve as a basis for future development of certain cytotoxic agents in clinical practices.

## Conclusion

All the newly synthesized Schiff bases ligands **L$^1$**–**L$^3$** act as tridentate ligands, and all these are coordinated through the azomethine-N, triazole ring —N and hydroxyl-O to the metal ion. All the synthesized metal(II) complexes possessed an octahedral geometry except the Cu(II) complexes which showed a distorted octahedral geometry. The findings of biological studies indicated that the Schiff base ligands possessed mostly moderate activity and metal(II) complexes mostly possessed moderate to significant activities against different bacterial and fungal strains which might be due to azomethine (—HC═N—) linkage and/or heteroatoms present in these compounds. The biological activity results showed that majority of the Schiff base ligands possessed increased activity upon coordination with different metalloelements. The improvement in biological activity upon coordination may be explained on the basis of Overtone's concept and chelation theory.

## Acknowledgements

The authors are grateful to Higher Education Commission (HEC), Government of Pakistan for the award to carry out this research. We are also thankful to HEJ research Institute of Chemistry, University of Karachi, Pakistan, for providing help in taking NMR, mass spectral and antibacterial/antifungal data.

## References

[1] I.A. Al-Masoudi, Y.A. Al-Soud, N.J. Al-Salihi, N.A. Al-Masoudi, Chem. Heterocycl. Compds. 42 (2006) 1377.
[2] T. Propst, W. Vogel, A. Propst, O. Dietze, H. Braunsteiner, J. Mol. Med. 70 (1992) 55–58.
[3] S.M. Stahl, CNS Spectr. 13 (2008) 1027–1038.
[4] G. Capranico, G. Zagotto, M. Palumbo, Curr. Med. Chem. Anticancer Agents 4 (2004) 335–345.
[5] A. Iqbal, H.L. Siddiqui, C.M. Ashraf, M. Ahmad, G.W. Weaver, Molecules 12 (2007) 245–254.
[6] K. Vashi, H.B. Naik, Eur. J. Chem. 1 (2004) 272–276.
[7] M.E. Hossain, M.N. Allam, J. Begum, M.A. Akbar, M.N. Uddin, F.E. Smith, R.C. Hynes, Inorg. Chim. Acta 249 (1996) 207–213.
[8] K.P. Sharma, V.S. Jolly, P. Phatak, Ultra. Sci. Phys. Sci. 10 (1998) 263–266.
[9] A.K. Sadana, Y. Mirza, K.R. Aneja, O. Prakash, Eur. J. Med. Chem. 38 (2003) 533–536.
[10] Z. Rezaei, S. Khabnadideh, K. Pakshir, Z. Hossaini, F. Amiri, E. Assadpour, Eur. J. Med. Chem. 44 (2009) 3064–3067.
[11] H. Guo-Qiang, H. Li-Li, X. Song-Qiang, H. Wen-Long, Chin. J. Chem. 26 (2008) 1145–1149.
[12] J. Jin, L. Zhang, A. Zhang, X.X. Lei, J.H. Zhu, Molecules 12 (2007) 1596–1605.
[13] G.B. Bagihalli, P.G. Avaji, S.A. Patil, P.S. Badami, Eur. J. Med. Chem. 43 (2008) 2639–2649.
[14] Z.H. Chohan, M. Hanif, Appl. Organomet. Chem. 25 (2011) 753–760.
[15] S.A. Rice, M. Givskov, P. Steinberg, S. Kjelleberg, J. Mol. Microbiol. Bio-technol. 1 (1999) 23–31.
[16] S.J. Lippard, J.M. Berg, Principles of Bioinorganic Chemistry, University Science Books, Mill Valley, CA, 1999.

[17] Z.H. Chohan, S.H. Sumrra, M.H. Youssoufi, T.B. Hadda, Eur. J. Med. Chem. 63 (2010) 3981–3998.
[18] D.M. Taylor, D.R. William, Trace Element Medicine and Chelation Therapy, The Royal Society of Chemistry, 1995.
[19] R.J.P. Williams, Metal ions in biological systems, Biol. Rev. (2008).
[20] Y. Lu, N. Yeung, N. Sieracki, N.M. Marshall, Design of functional metalloproteins, Nature (2009).
[21] A.U. Rahman, M.I. Choudhary, W.J. Thomsen, Bioassay Techniques for Drug Development, Harwood Academic Publishers, The Netherlands, 16, 2001.
[22] J.L. McLaughlin, C.J. Chang, D.L. Smith, In: Atta-ur-Rahman (Ed.), Studies in Natural Products Chemistry, "Bentch-Top" Bioassays for the Discovery of Bioactive Natural Products: An Update, Structure and Chemistry (Part-B). The Netherlands, Elsevier Science Publishers, vol. 9, 1991, p. 383.
[23] D.J. Finney, Probit Analysis, 3rd ed., Cambridge University Press, 1971.
[24] B.N. Meyer, N.R. Ferrigni, J.E. Putnam, L.B. Jacobsen, D.E. Nichols, J.L. McLaughlin, Planta Med. 45 (1982) 31–42.
[25] G.B. Bagihalli, P.S. Badami, S.A. Patil, J. Enz. Inhib. Med. Chem. 23 (2008) 1–14.
[26] Z.H. Chohan, S.H. Sumrra, M.H. Youssoufi, T.B. Hadda, J. Coord. Chem. 63 (2010) 3981–3998.
[27] Y. Prashanthi, S. Raj, J. Sci. Res. 2 (2010) 114–126.
[28] R. Freeman, A Handbook of Nuclear Magnetic Resonance, 2nd ed., Longman Publishing, 1997.
[29] M. Levitt, Spin Dynamics: Basics of Nuclear Magnetic Resonance, John Wiley and Sons, 2001.
[30] Y.M. Issa, H.B. Hassib, H.E. Abdelaal, Specchim. Acta Part A 74 (2009) 902–910.
[31] D.J. Harvey, J. Am. Soc. Mass Spectrum. 11 (2000) 900–915.
[32] W.J. Geary, Coord. Chem. Rev. 7 (1971) 81–121.
[33] C.J. Balhausen, An introduction to Schiff bases field. McGraw Hill, New York, 1962.
[34] K. Serbest, H. Kayi, E. Mustafa, K. Sancak, I. Degirmencioglu, Heteroatom. Chem. 19 (2008) 700–712.
[35] Z.H. Chohan, Trans. Met. Chem. 34 (2009) 153–161.
[36] A.B.P. Lever, Inorganic Electronic Spectroscopy, Elsevier, New York, 1984.
[37] B.S. Creaven, M. Devereux, A. Foltyn, S. McClean, G. Rosair, V.R. Thangella, M. Walsh, Polyhedron 29 (2010) 813–822.
[38] Z.H. Chohan, S.H. Sumrra, J. Enz. Inhib. Med. Chem. 25 (2010) 599–607.
[39] D.P. Singh, K. Kumar, R.M. Chopra, Specchim. Acta Part A 78 (2011) 629–634.